WETTING PHENOMENA OF GROOVES AT LIQUID METAL/CERAMICS INTERFACE

The grain boundary groove (GBG) developing at the ceramic substrate under the liquid metal is evident, yet not fully explained influencing appearance in describing the wetting phenomena at liquid metal/ceramics interface. The focus here is on modelling of the phenomena at/around a groove between grains depending on grooves' geometry. Based on atomic force microscopy results, the groove efficiency assessment is provided as a function of the transferred mass quantity and related to grooves geometry. The transferred mass quantity and, according to it, the groove efficiency at parabolic GBG is about 10 % higher comparing to the triangular GBG.

Key words: liquid metal, ceramics, interface, grain boundary grooves, wetting

INTRODUCTION

The wetting phenomena are important for understanding the metal/ceramics joining process and further process development. The liquid metal/ceramic substrate systems can be encountered from metals processing, tools manufacturing, in high temperature and corrosion protection applications, in automotive industry and especially in microelectronics [1-7]. Despite developed practical applications, the interface bonding of these two juxtaposed components is not fully explained yet. 'Reaction product control' theory claimed that the interface reactions take control over the wetting mechanism at interface [8,9]. The other theory stated that capillary effects and adsorption of metals onto the ceramic substrate with triple line ridging are crucial for controlling the wetting phenomenon, not chemical reactions [1,2]. Properties of the resulting metal/ceramic interface extremely depend on the thickness, uniformity and porosity of the bonding layer, which may be the result of non-homogeneous chemical transformation that starts at the ceramic surface and propagates into the liquid metal [5-7,10,11].

Lattice matching of the two adjacent materials is another significant factor governing characteristics of the reaction layer formation at metal-ceramic interface [11-13].

So-called surface topography, such as roughness and other irregularities on the macroscale, or grain boundary grooves (GBG) and lattice pits at microscale, significantly modifies properties of the liquid metal/solid ceramic interface. Finally, aside of the reactive or non-reactive wetting, it is influenced by the mechanisms occurring at nanoscale [14-18].

M. Mihailović, A. Patarić, Z. Gulišija, ITNMS, Belgrade, K. Raić, Faculty of Technology and Metallurgy, Belgrade, Serbia

Experimental studies of wetting phenomena on substrates patterned by pits, grooves and wedges with finite depths show the strong influence of nanostructure on the adsorption behaviour, comparing to that on flat substrates [14]. It is stated that the classical contact angle considerations were invalid for the tip of a spreading film. The shape, size and layout of the grain boundary grooves (GBG) grooves should be taken into account.

MODEL OF GBG WETTING

The phenomena at grain boundary grooves (GBG) on metal/ceramic interface are presented here as an original theory, encompassing the geometry of grooves influence on mass transport. In modelling GBG processes here, the analogies between mass and heat transfer, according to the transport phenomena standpoint, are applied [19].

Due to the capillary forces, the leading edge of the liquid droplet develops a ridge at the solid–liquid–vapour triple junction, recorded in several metal-ceramic systems using AFM [1]. Grain boundary grooving is enhanced in the area under the liquid, and the groove cross-sections of interest are parabolic or triangular, according to recorded AFM profiles [4].

Having in mind the analogies between mass and heat transfer, a mathematical analysis similar to the extended surfaces modelling is applied here [20]. The generalized differential equation for the groove concentration profile is expressed based on consideration of the steady-state mass balance over the differential element of the groove depth dy, with planes parallel to the groove base at y and $y+dy$, (Figure 1). Here, y is a distance from the groove tip to an observed element of the groove depth. The limiting profile curves are expressed as $x = \pm f_2(y)$.
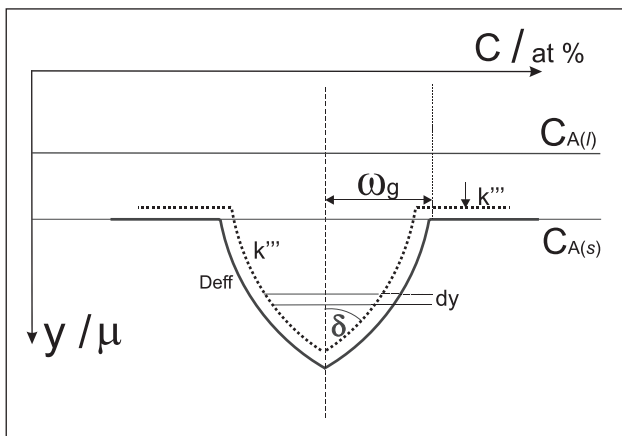
Figure 1 Parabolic type of a grain boundary groove

Where:
- $C_{A(l)}$ – is the concentration in liquid metal
- $C_{A(s)}$ – is the concentration in solid ceramics
- D_{eff} – the effective diffusion coefficient from the liquid metal into the porous solids
- k''' – is the surface rate constant
- k_m – is the mass transfer coefficient
- u – the groove perimeter
- L_g – the groove length
- ω_g – the groove half-width
- ϑ – is excess of concentration between a point on the groove and the surroundings.

To meet the terms of a steady state, the difference in mass transfer into and out of the element dy, must be balanced by mass dissipation from the lateral surface of the groove. This also postulates that the element dy on a random surface described by function $f_2(y)$ is equal in height to the element dy on the y-axis.

The mass difference (dm) caused by the mass entering the observing element by diffusion at $y + dy$ and the mass leaving the GBG element by diffusion at y is:

$$dm = D_{eff} \frac{d}{dy}\left[f_1(y) \frac{dC_A}{dy} \right] \qquad (1)$$

For $\vartheta = C - C_{A(S)}$ and because of $C_{A(S)}$ is assumed to be constant, it follows $d\vartheta = dC$.

When $k''' <<< k_m$, than the k''' becomes rate limiting constant, and since both have the same dimension, k''' should substitute k_m, giving the following:

$$dm = k''' u\, (C - C_{A(S)})\, dy \qquad (2)$$

or

$$dm = 2\, k'''[L_g + f_2(y)](C - C_{A(S)}) \qquad (3)$$

Here is to be applied the Murray–Gardner assumption, which states that the groove depth must be small in comparison to its length, $L_g >> 2f_2(y)$. Hence:

$$dm = 2k'''L_g(C - C_{A(S)})dy \qquad (4)$$

Equating the equations (1) and (4), the general differential equation is obtained:

$$f_1(y) \frac{d^2\vartheta}{dy^2} + \frac{df_1(y)}{dy}\frac{d\vartheta}{dy} - \frac{2k''}{D_{eff}}\vartheta = 0 \qquad (5)$$

The profile function $f_2(y)$, for any longitudinal groove is in the following form:

$$f_2(y) = \omega_g \left(\frac{y}{l} \right)^{\frac{1-2n}{1-n}} \qquad (6)$$

For parabolic groove profile, the exponent here satisfies the groove geometry for n = 1/3, while for triangular GBG cross-section, the exponent satisfies geometry when n = 0.

Introducing z, the groove performing parameter:

$$z = (k'''/D_{eff}\omega_g)^{1/2} \qquad (7)$$

and substituting it in eqn. (5), together with adequate profile function $f_2(y)$, and the groove depth l, the governing differential equation for parabolic GBG profile for concentration excess $\vartheta(y) = C(y) - C_{A(S)}$, turns into:

$$\sqrt{y}\frac{d^2\vartheta}{dy^2} + \frac{1}{2\sqrt{y}}\frac{d\vartheta}{y} - z^2\sqrt{l}\,\vartheta = 0 \qquad (8)$$

while for triangular GBG profile it is as follows:

$$y\frac{d^2\vartheta}{dy^2} + \frac{d\vartheta}{dy} - z^2 l\vartheta = 0 \qquad (9)$$

RESULTS AND DISCUSSION

Calculation of the transferred mass quantity for each GBG starts by differentiating the equation for the particular solution and evaluating the derivative at $y = l$. Designating the groove cross-section with $S = \omega_g L_g$ and applying expanded Bessel function for according to [20], the mass quantity transferred through the groove of a parabolic profile is:

$$m_l = D_{eff} \frac{\omega_g}{2} L_g z \vartheta_l \frac{I_{2/3}\left(\frac{4}{3}zl\right)}{I_{-1/3}\left(\frac{4}{3}zl\right)} \qquad (10)$$

Accordingly, the mass quantity transferred through the groove of a triangular profile is:

$$m_l = D_{eff} S \frac{dC}{dy}\bigg|_{y=l} = \frac{2k''L_g\vartheta_l I_1(2zl)}{zI_0(2zl)} \qquad (11)$$

Where:
- l – is the groove depth
- I_0 – modified Bessel function of the first kind
- I_n – modified Bessel function for different profile function exponent n, eqn. (6)

The groove efficiency is the ratio of the actual and the ideal mass transfer, $m_{ideal} = 2k'''lL_g\vartheta_l$, so:

$$\eta = \frac{2k''L_g\vartheta_l\left[(2zl)/zI_0(2zl)\right]}{2k''lL_g\vartheta_l} \qquad (12)$$

The zl parameter, which figures in both equations, for the quantity of mass transferred through the groove and for the groove efficiency, encompasses the groove dimension and mass transfer influence.
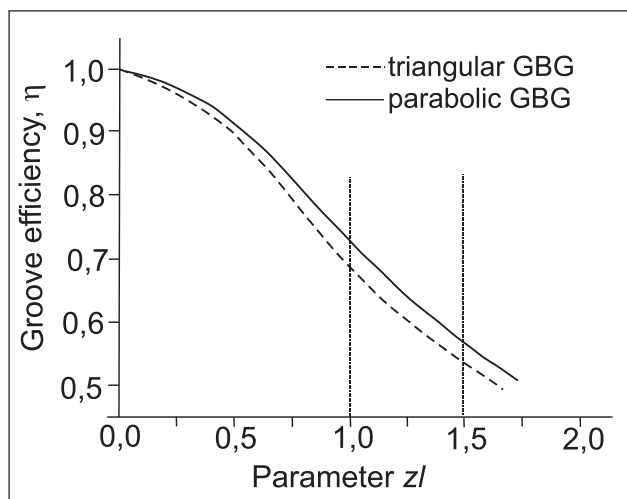
Figure 2 Groove efficiency η vs. zl parameter, for both groove profiles

The groove mass transfer as well as the groove efficiency are related to groove perform parameter z, directly depending on the grooves geometry, eqn. (7). When k''' and D_{eff} are constant in a particular system, the groove efficiency is influenced by GBG geometry. Observing GBG profiles obtained using atomic force microscopy (AFM) and measurements of grooves by high resolution scan in the Ni/Al_2O_3 system [4], the calculations can be performed according to the here proposed model of GBG wetting.

For the surface rate constant estimated to be $k'''{\sim}10^{-5}$ m/s in this system [4], it is calculated that $\omega_g D_{eff} = 4,4 \cdot 10^{-19}$ m³/s.

Since the measured groove depth is $l = 0,2$ μm $= 2 \cdot 10^{-7}$ m [4], the groove performing parameter from eqn. (7) can be determined. Upon calculation, $zl \approx 1$ is obtained.

According to the reported AFM profiles, the cross-section of the GBG can vary in shape. The groove efficiency for both characteristic types of groove profiles, triangular and parabolic, using the proposed calculation is presented (Figure 2).

It can be concluded that the maximum difference in groove efficiency between these characteristic groove types is at/around the value 1 for zl parameter, which is previously calculated based on the value of groove performing parameter z.

Observing the dependence of groove efficiency for both characteristic types of grain boundary groove profiles on zl parameter, it can be concluded that the maximum difference in groove efficiency between these characteristic groove types is at/around the value 1 for zl parameter, which is calculated based on the value of groove perform parameter z.

It is evident that groove efficiency, η, strongly depends on the groove profile. The efficiency of triangular GBG is below the parabolic value. The quantity of mass transferred through parabolic GBG is about 10 % higher comparing to the mass transferred through triangular GBG.

Since the groove perform parameter z, directly depends on the groove geometry, eqn. (7), it can be noted that with groove width decrease or depth increase, the zl parameter increases, reaching its maximum influence in the interval between 1 and 1,5 (Figure 2). The difference in groove efficiency for different grooves geometry, when zl parameter reaching value 0, is becoming less influential, meaning that with very wide grooves or small groove depth, the surface is becoming almost flat.

With zl parameter increasing, the difference between characteristic groove profiles increases, and for $zl > 0,2$ the groove geometry influence is evident.

The calculation has proven the prediction of the GBG wetting model, i.e. that grooves efficiency, η, strongly depends on the grooves profile. The efficiency of triangular GBG is below the parabolic value. The quantity of mass transferred through parabolic GBG higher comparing to the mass transferred through triangular GBG, implying that the groove efficiency, as well as liquid metal/ceramic joining can be influenced by GBG geometry.

CONCLUSIONS

The wetting phenomena at liquid metal / ceramics interface are shown to be the GBG geometry dependent. Grain boundary grooves are, according to reported AFM profiles, classified as triangular or parabolic and completely evaluated from the governing differential equation, to groove efficiency, η. The calculated values, according to the analytical model, reveal evident differences between profiles, giving the higher groove efficiency for parabolic profile and its maximum influence for parameter $zl \approx 1$.

Based on AFM measurements, the calculated groove efficiency for parabolic GBG is about 10 % higher comparing to the triangular GBG. The quantity of mass transferred through parabolic concave GBG is, according to proposed equations, proportional to the grove efficiency.

This implies that the metal/ceramic joining process can be influenced by GBG geometry.

Acknowledgements

REFERENCES

[1] E. Saiz, R.M. Cannon, A. P. Tomsia, Reactive spreading: adsorption, ridging and compound formation, Acta Materialia 48 (2000) 4449–4462. doi:10.1016/S1359-6454(00)00231-7

[2] E. Saiz, A. P. Tomsia, R. M. Cannon, Triple line ridging and attachment in high-temperature wetting, Scripta Materialia 44 (2001) 159–164. doi:10.1016/S1359-6454(00)00231-7

[3]   C. Rado, S. Kalogeropoulou, N. Eustathopoulos, Bonding and wetting in non-reactive metal:SiC systems: weak or strong interfaces?, Material Science and Engineering A, 276 (2000) 195–202. doi:10.1016/S0921-5093(99)00274-9

[4]   E. Saiz, R.M. Cannon, A.P. Tomsia, Energetics and atomic transport at liquid metal/Al2O3 interfaces, Acta Materialia 47 (1999) 15, 4209-4220. doi:10.1016/S1359-6454(99)00279-7

[5]   S-I Tanaka, C. Iwamoto, Nanoscale dynamic wetting and spreading of molten Ti alloy on 6H–SiC, Material Science and Engineering A, 495 (2008) 168–173. doi:10.1016/j.msea.2007.11.096

[6]   G. Elssner, G. Petzow, Metal/ceramic joining, ISIJ International 30 (1990) 1011-1032. doi: 10.2355/isijinternational.30.1011

[7]   F. Spaepen, Interfaces and stresses in thin films, Acta Materialia 48 (2000) 31-42. doi:10.1016/S1359-6454(99)00286-4

[8]   B. Drevet, K. Landry, P. Vikner, N. Eustathopoulos, Influence of substrate orientation on wetting kinetics in reactive metal/ceramic systems, Scripta Materialia 35 (1996) 1265-1270. doi:10.1016/1359-6462(96)00305-3

[9]   C. Rado, B. Drevet, N. Eustathopoulos, The role of compound formation in reactive wetting: the Cu/Sic system, Acta Materialia 48 (2000) 4483–4491. doi:10.1016/S1359-6454(00)00235-4

[10]   K.T. Raic, An estimate of Si3N4 diffusion into Cu based filler metal, Ceramics International 26 (2000) 19-24. doi:10.1016/S0272-8842(99)00013-9

[11]   C. Iwamoto, S-I. Tanaka, Atomic morphology and chemical reactions of the reactive wetting front, Acta Materialia 50 (2002) 749–755. doi:10.1016/S1359-6454(01)00388-3

[12]   G.W. Liu, M.L. Muolo, F. Valenza, A. Passerone, Ceramics International 36 (2010) 1177-1188. doi:10.1007/s10853-009-3858-0

[13]   M. Mihailović, K. Raić, A. Patarić, T. Volkov-Husović, Survey on wetting of SiC by molten metals, Materials and technology 49 (2015) 3, 413-416. doi:10.17222/mit.2014.111

[14]   M. Tasinkevych, S. Dietrich, Complete wetting of pits and grooves, European Physical Journal E, 23 (2007) 117–128. doi: 10.1140/epje/i2007-10184-5

[15]   M.W. Finnis, The theory of metal–ceramic interfaces, Journal of Physics: Condensed Matter 8 (1996) 5811-5836. doi:10.1088/0953-8984/8/32/003

[16]   T. Hofmann, M. Tasinkevych, A. Checco, E. Dobisz, S. Dietrich S, B.M. Ocko, Wetting of nanopatterned grooved surfaces, Physical Review Letters 104 (2010) 106102. doi:10.1103/PhysRevLett.104.106102

[17]   K.T. Raic, Unsteady or starting phenomena at liquid metal/ceramic interfaces, Advances in Science and Technology 32 (2003) 725-733.

[18]   M. Mihailović, T. Volkov-Husović, K.T. Raić, Micro- and nano-scale wetting of reactive metal at metal-ceramic interface, Advances in Science and Technology 45 (2006) 1526-1531. doi:10.4028/www.scientific.net/AST.45

[19]   J.R. Welty, C.E. Wicks, R.E. Wilson, Fundamentals of momentum, heat and mass transfer, John Wiley and Sons, New York, 1984, pp.339-599

[20]   A.D. Kraus, A. Aziz, J. Welty, Convection with Simplified Constraints. In: Extended Surface Heat Transfer, John Wiley & Sons, Inc, Hoboken, NJ, USA, 2000, pp.1-57. doi: 10.1002/9780470172582.ch1

Note: The responsible translator for English language is certified translator from the Association of Scientific and Technical Translators of Serbia